Dynamic Material Model of Annealed Soda-lime Glass

Xihong Zhang[1]* and Hong Hao[2]

1. School of Civil and Resource Engineering, the University of Western Australia

35 Stirling Highway, Crawley WA 6009, Australia

2. Tianjin University and Curtin University Joint Research Center for Structure Monitoring and Protection, School of Civil and Mechanical Engineering, Curtin University, Kent Street, Bentley WA 6102, Australia

email: xihong.zhang@uwa.edu.au

Phone: +61 8 6488 7199

Abstract

Glass is an omnipresent material which is widely used as façade in buildings. Damage of glass windows and the associated glass fragments induced by impact and blast loads impose great threats to people in the vicinity. Much effort has been directed at understanding glass material properties, and modeling of glass window responses to impact and blast loads. For reliable predictions of glass structure performances under dynamic loadings, an accurate dynamic constitutive model of annealed float glass, which is commonly used for glass windows, is therefore needed. In current practice, the Johnson-Holmquist Ceramic (JH2) model is most commonly used in simulating glass plate responses to impact and blast loads. In this study, the accuracy of the JH2 model in modeling annealed float glass material, especially at high strain rate is examined in detail. Static compressive tests and dynamic compressive tests using Split Hopkinson Pressure Bar (SHPB) are carried out on soda-lime glass specimens sampled from commercially used annealed float glass panels. These testing results are used together with the authors' previous testing data and data reported by other researchers in the literature to determine the constitutive constants for the JH2 model, including Equation of State (EOS), strength criterion and strain-rate effect. The JH2 model with new material constants is then programmed in commercial code LS-DYNA. To verify the

model, it is used to simulate a SHPB compressive test on a 15mm by 15mm (diameter by length) glass specimen, a field blast test on a laminated glass window of 1.5m by 1.2m in dimension, and a full-scale laboratory windborne debris impact test on a laminated glass window. The simulation results demonstrate that the JH2 model with the new material constants for annealed glass gives good predictions of glass material and glass window responses to impact and blast loads.

KEYWORDS: dynamic material model; annealed float glass; soda lime; Johnson Holmquist Ceramic model; high strain rate; blast; impact

1 INTRODUCTION

Annealed soda-lime glass is an omnipresent construction material that has been widely used for windows and façade in buildings. Due to its relatively low strength and brittleness, glass is very fragile especially in face of extreme loads, such as shock and impact loads. Under impact and blast loads the fractured annealed glass, which is jagged and flying at high velocity, could cause enormous casualties. Post-event investigations on terrorist bombing attacks, accidental explosions and cyclone induced debris impact have cited the fractured glass façade and windows as a major threat to the safety of structures and residents. For instance, in the Norway attacks in 2011, the shock wave from the car bomb shattered almost all the windows of the Oslo executive government building. 209 victims out of the total 325 injuries were associated with glass laceration [1]. Similarly, after the 1974 cyclone Tracy, the post-event investigation concluded that one of the most remarkable factors contributing to the wide scale overturning and damage of houses was the overwhelming internal pressure following the windward window failure due to windborne debris impact [2]. A number of studies have been carried out to analyze the responses of glass windows under such extreme loading conditions [3-8], and to seek respective retrofit techniques [3, 9]. Nevertheless, there is still a lack of integrated and systematic study on annealed glass dynamic material properties and development of dynamic material models to simulate glass

window response. Consequently, many previous studies could only adopt static material model, which left the accuracy of results in doubt [5, 6]. Therefore, to better analyze and design glass windows for personnel and property protection, it is necessary to more thoroughly understand glass dynamic material properties, which will lead to better analysis and prediction of glass window behavior against impact and blast loads.

Glass is an idealized isotropic and brittle material. However, variations in its chemical compositions and manufacturing processes lead to diversified glass material characteristics and properties. Glass is produced by heating a mixture of raw minerals above a transition point. The molten glass is then floated on top of molten tin after which it is slowly cooled without quenched in the annealing lehr. Soda-lime glass commonly used for structural glass windows is mainly made of SiO_2 (about 50~75% mass proportions). Comparatively, borosilicate glass with higher SiO_2 ratio is normally stronger and has better temperature shock resistance, which is often chosen for reagent. Manufacturing processes also lead to various glass strengths and fracture characteristics. For instance, the standard float process produces annealed glass, which is very low in strength and breaks into large jagged shards with sharp ends. By heating and quickly cooling annealed glass yields heat strengthened glass, which leads to higher strength. Uniformly heating annealed glass to a temperature of up to 700˚C and immediately cooling it produces fully tempered glass, which has very high strength as a result of the pre-stress introduced to glass during tempering process. Tempered glass is generally four to five times stronger than annealed glass. It also shatters into numerous fine pieces, which is comparatively less threatening. Despite the advantages of heat strengthened and tempered glass, due to its low cost annealed soda-lime glass has been ubiquitously used for structural glass windows. Considering the overwhelming usage in building structures and serious consequences that always leads to mass injuries, the current study focuses on the investigation of annealed soda-lime glass.

Recently, many researches have been directed towards fully unveiling the dynamic behavior of different types of glasses. For instance, the dynamic deformation and fracture behavior of borosilicate glass with confined or unconfined stresses were investigated intensively [10-14]. Strain-rate effect and surface condition influences on the borosilicate glass strength were evaluated experimentally [15]. Similarly, for soda-lime glass, the fracture process and densification behavior under shock load were investigated thoroughly through plate impact tests [16-19]. The dynamic increment effect on uniaxial compressive strength and split-tensile strength (determined by splitting a cylinder across the diameter, also known as the Brazilian test) of soda-lime glass were recently studied [20, 21]. The studies demonstrated that glass behaves very differently under dynamic and static loadings. Like other construction materials such as concrete and steel, glass is also strain-rate sensitive. Its ultimate strength is amplified when deformation rate is significant. Bulk damage could be triggered by high intensity stress under dynamic loading, where the influence of glass surface flaw is less prominent because there is limited time for cracks to find the relatively weaker sections to develop [21]. Both the compressive and tensile dynamic increment factors (DIF), which are the ratio of dynamic ultimate strength to the corresponding static ultimate strength, are determined with respect to the strain rates the tested glass specimen experienced. Using a modified SHPB device, Zhang et al. [21] performed dynamic compressive tests on annealed glass at the strain rates from $98s^{-1}$ to $376s^{-1}$. A bi-linear relation between glass compressive DIF and strain rate was found. In the same study, tensile tests carried out through split-tensile test found a similar trend on the tensile DIF vs. strain rate relationship. It should be noted that in determining the glass material constants of JH2 model, compressive tests were conducted at two strain rates only, while split-tensile tests were only performed at static state [22]. The lack of dynamic tensile tests was mainly because the results were used to model glass ballistic performance, where glass tensile strength was considered less crucial. However, when modeling thin glass panel response to

lateral loads, glass tensile strength will strongly influence the glass panel behavior. A better strength model for glass in the tensile region is deemed necessary. With more and more thorough studies on annealed glass dynamic compressive and tensile strengths at various strain rates, modification and determination of updated constants of JH2 model for annealed glass can be achieved to better model the glass behavior, especially for glass windows subjected to impulsive lateral loads.

Most previous researches on soda-lime glass showed that the glass is capable of bearing over 1.0GPa uniaxial compressive stress [20, 22]. The split-tensile strength of float glass in JH2 model is also well over 100MPa [22]. These results were found inconsistent with some recent experiment results on annealed soda-lime glass [21]. The discrepancy is believed to be attributed to differences in sample surface conditions. As pointed out by Nie et al. [15] that glass strengths exceeding 1.0GPa were produced by submersing the specimens in acid fluid to blunt out surface cracking. This could be suitable for transparent armor for military purpose but is not a process in producing the construction glass panels. Therefore, existing material constants for annealed soda-lime glass overestimates the material strengths of glass commonly used for windows. To better predict the glass window responses, modifications of material constants are therefore required for JH2 model.

Based on the experimental tests, some glass dynamic material models have been developed. These models could be categorized into three levels: micro-level (molecular) model [23]; explicit crack model [24]; and macro-level (continuum) model. Considering computational efficiency, the first two categories are less suitable for studying full-scale glass windows. Therefore they are not elaborated herein. Based on glass flaw distribution, Grujicic et al. [25] formulated a continuum level glass model for ballistic impact. The idea of shielding zone was introduced as glass damage propagates. However, this model is less suitable in simulating thin glass panel under lateral loads. Johnson-Holmquist Ceramic (JH2)

model [22] for float glass is another macro level model, which was developed in early 1990's. JH2 model is a well-defined material model which considers strain-rate effect, material damage and also confinement effect. It has been popularly used in simulating glass response to shock and impact loads [3, 26]. Modifications of the original JH2 model have been made over the years to improve the adaptability for different types of brittle materials. For instance, by conducting laboratory and ballistic experiments, Holmquist et al. [27] determined the material constants explicitly for aluminum nitride (AlN). The original JH2 model was later modified with the capability of phase change so as to better model the behavior of AlN [28]. For glass material, Holmquist and Johnson [29] related material strength to its location (in the interior, on the surface or adjacent to failed material) and surface condition. They also included thermal softening, damage softening, and time-dependent softening, etc. into the modified model. These new features were illustrated to provide better predictions of glass response under ballistic impact. Nevertheless, these improvements are not necessarily crucial to model the behavior of architectural glass windows under relatively low speed impact and blast loading. The complexity of the above modification requires more computational resources. Considering the fact that the original JH2 model is well understood and overwhelmingly used, and has also been implemented in many commercial codes, such as LS-DYNA, conducting laboratory tests on low strength architectural annealed glass and determining new material constants for JH2 model for better prediction of architectural annealed glass window responses to impact and blast loading is important.

In this study, compressive SHPB tests were further carried out on glass specimens sampled directly from commercially used window glass sheets. Experimental data together with those obtained in the previous tests [21] and available testing data reported by other researchers in the literature are used to derive material constants for JH2 model. To verify the accuracy of the model with the updated material constants, it is used to simulate a

compressive SHPB test on a 15mm × 15mm glass specimen, a field test of glass windows subjected to blast loads, and a full-scale laboratory test on glass windows subjected to windborne debris impact. Numerical simulation results are compared with the testing data. The comparisons demonstrate that the JH2 model with the newly determined constants for architectural annealed glass gives reliable predictions of glass responses to impact and blast loads.

2 EXPERIMENTAL INVESTIGATIONS ON GLASS MATERIAL PROPERTIES

Recent laboratory tests on annealed soda-lime glass specimens, which were sampled directly from as-received commercial glass sheet without any post-processing treatment, reported significant differences in glass static and dynamic ultimate strengths for both tension and compression [21] from those used to determine JH2 model constants for float glass [22]. A significant variation was also reported on glass dynamic increment factor (DIF). Owing to the equipment limitation, the previous laboratory tests were only able to reach a strain rate up to about $800s^{-1}$. To determine glass material behavior in higher strain rate range, and also to further verify the observed data and discrepancy with those in reference [22], further static and dynamic compressive tests were carried out in this study using a smaller diameter Split Hopkinson Pressure Bar device. For consistency, same glass specimens were used in the current tests as in [21].

2.1 Quasi-static test

The glass specimens were provided by Australian glass supplier Viridian®. As described in reference [21], 15mm thick annealed glass sheet (soda-lime) for general window purposes were cut into square pieces, and then ground into 15mm diameter glass cylinders as shown in Figure 1. No special surface treatment was performed to glass specimens. Quasi-static compression tests were firstly performed using INSTRON hydraulic testing machine (Figure 2). The compression speed of the machine crosshead was controlled at 0.12mm/min, which led to a strain rate of $1.33e\text{-}4s^{-1}$ on the glass specimens. The top and bottom surfaces of the

glass specimens were lubricated to reduce friction effect. The specimens were compressed till failure. Load cell was used to measure the applied compressive load. A strain gauge was mounted to the vertical surface of each specimen to track the axial strain. Stress-strain curves of three specimens tested are shown in Figure 3. It can be observed that under quasi-static compression, annealed glass has almost a linear stress-strain relation until fracture. The ultimate compressive strengths were reached when brittle failure occurred. Table 1 lists the ultimate true compressive strength and Young's modulus. It is worth noting that the averaged static true compressive strength is about 237MPa, which is consistent with the testing results in reference [21], but lower than those used for determination of JH2 constants. Therefore, modification on material strength constants in JH2 model is necessary before applying it to analyze annealed glass panel responses to impact and blast loads.

2.2 Dynamic test

2.2.1 Experimental procedure and results

Dynamic compressive tests were conducted on SHPB instrument with a 20mm diameter incident and transmitter bars (Figure 4). The bars are made of maraging steel. Bar density and Young's modulus are 8100kg/m^3 and 210GPa, respectively. As a result of larger specimen diameter to bar diameter ratio, higher strain rates were achieved in this new set of dynamic tests as compared to those reported in [21]. Strain gauges were mounted to the middle of the incident bar and the transmitter bar to track the stress waves. A strain gauge was glued to the surface of the specimen to measure the strain. Figure 5 shows the typical stress wave signals recorded on the incident and transmitter bars. A 2mm thick copper pulse shaper was placed on the impact surface of the incident bar in order to shape the incident pulse. Stress equilibrium is carefully checked for each test. Results from 10 tests, which satisfy equilibrium, are identified and used in the present study. They have strain rates in the range between 619s^{-1} and 1465s^{-1}. Together with the previous testing data, a wider strain-

rate range is covered for modelling glass dynamic material strength. Figure 6 shows the typical true stress-strain curves of glass at various strain rates.

2.2.2 Analysis and discussion

The newly tested glass dynamic true compressive strengths (Table 2) are normalized against the averaged static true compressive strength, so as to derive the compressive DIFs. Together with the DIF data reported in reference [21] and the testing data used for the original JH2 model [22], the compressive DIFs are plotted versus strain rates in Figure 7a. As can be observed, the new testing data show a consistent trend as those reported before, which reinforce the empirical formula derived in reference [21]. As shown glass compressive DIF grows slowly as strain rate increases in quasi-static and low strain rate region, but increases quickly when strain rate is above $100s^{-1}$. A very significant difference can be found between the DIF data used in the original JH2 model and the newly tested data. The difference could be attributed to two reasons: firstly, the chemical compositions of the two kinds of float glass differ. The amount of SiO_2 plays a vital role in the material properties, especially glass compressive and tensile strengths. The float glass tested by Holmquist et al. [22] comprises about 74% of SiO_2, whereas due to environmental consideration, less sand is mixed into glass raw composites nowadays which leads to a low percentage of SiO_2 (about 51%). With lower SiO_2 percentage, the architectural annealed glass has lower strength and exhibits a different DIF vs. strain rate relationship. Secondly, surface treatments on the glass specimens could be different. As described above, the glass cylinders herein was ground from float glass sheet without acid blunt or fine surface polishing, while the surface condition of the glass specimen in reference [22] was not specifically stated. Since the glass in reference [22] was tested in ballistic impact and its compressive strength was over 1GPa, it is believed that the glass was probably used for military armor and had gone through surface treatment. With testing data at only two strain rates, i.e. quasi-static ($10^{-3}s^{-1}$) and $250s^{-1}$, the DIF relation with respect to strain rate in the original JH2 model is therefore

linear, which is very different from what is derived from the recent testing data. Moreover, it can be noted that at strain rate 250s^{-1}, the DIF of the current data is higher than that used in the original JH2 model. This comparison demonstrates again the need to revise the strain rate and material strength constants in the original JH2 model for float glass used for common glass windows.

3. DETERMINATION OF MATERIAL CONSTANTS

The JH2 model was proposed by Johnson and Holmquist [30] to simulate the ballistic performance of ceramic materials. This model consists of a strength model, a damage model, a model for strain-rate effect, and an equation of state. Assessment and determination of material constants for annealed soda-lime glass are performed herein.

3.1 Strength model

The strength model of JH2 considers both the intact strength and material strength at fracture. A damage scalar is introduced to represent the transition from the intact to the fractured state. The normalized equivalent strength is calculated by

$$\sigma^* = \sigma^*_{\mathrm{i}} - \mathrm{D}(\sigma^*_{\mathrm{i}} - \sigma^*_{\mathrm{f}}) \tag{1}$$

where σ^*_{i} is the normalized intact strength, σ^*_{f} is the normalized material strength at fracture, and D is the damage scalar ($0 \leq \mathrm{D} \leq 1$). All the normalized stresses have the general form of $\sigma^*_{\mathrm{i}} = \sigma/\sigma_{\mathrm{HEL}}$, where σ_{HEL} is the equivalent stress at Hugoniot Elastic Limit (HEL), and σ is the actual equivalent stress with the general form of

$$\sigma = \sqrt{\frac{1}{2}\left[\left(\sigma_x - \sigma_y\right)^2 + \left(\sigma_x - \sigma_z\right)^2 + \left(\sigma_z - \sigma_y\right)^2 + 6\left(\tau_{xy}^2 + \tau_{xz}^2 + \tau_{yz}^2\right)\right]} \tag{2}$$

The normalized intact strength and material strength at fracture with strain-rate effect are given by

$$\sigma^*_{\mathrm{i}} = \mathrm{A}(\mathrm{P}^* + \mathrm{T}^*)^{\mathrm{N}}(1 + \mathrm{C}\ln\dot{\varepsilon}^*) \tag{3}$$

and

$$\sigma^*_{\mathrm{f}} = \mathrm{B}(\mathrm{P}^*)^{\mathrm{M}}(1 + \mathrm{C}\ln\dot{\varepsilon}^*) \tag{4}$$

where A, B, C, M, N and T are material constants; P^* stands for the normalized pressure ($P^*=P/P_{HEL}$), where P is the actual pressure and P_{HEL} is the pressure at HEL. Similarly, T* is the normalized maximum tensile hydrostatic pressure ($T^*=T/P_{HEL}$). $\dot{\varepsilon}^*$ is the actual strain rate over the reference strain rate ($\dot{\varepsilon}^* = \dot{\varepsilon}/\dot{\varepsilon}_0$,where $\dot{\varepsilon}_0 = 1.0\ s^{-1}$). The equivalent strain rate is expressed as

$$\dot{\varepsilon} = \sqrt{\frac{2}{9}\left[\left(\dot{\varepsilon}_x - \dot{\varepsilon}_y\right)^2 + \left(\dot{\varepsilon}_y - \dot{\varepsilon}_z\right)^2 + (\dot{\varepsilon}_z - \dot{\varepsilon}_x)^2 + \frac{3}{2}\left(\dot{\gamma}_{xy}^2 + \dot{\gamma}_{yz}^2 + \dot{\gamma}_{xz}^2\right)\right]} \quad (5)$$

In developing the original JH2 model, Holmquist et al. conducted static split tension, static and dynamic uniaxial compression tests to determine glass intact strength constants [22]. Following Holmquist et al.'s approach, testing results obtained in the present study together with the previous testing data reported in reference [21] on annealed glass are plotted in Figure 8. It is to mention that in the original JH2 model, the equivalent strength and the corresponding pressure need to be respectively normalized by σ_{HEL} and P_{HEL} at HEL, the compressive stress and pressure under uniaxial strain where the shock wave exceeds material elastic limit. Normally HEL is obtained through plate impact test. No plate impact test was performed by the authors on architectural float glass at HEL. Since the current work concentrates on architectural annealed glass and glass material strength is influenced by many factors, such as surface condition and treatment, chemical composition etc., to avoid misinterpretation of previous testing results on HEL for various glass material, a pseudo HEL is introduced herein, which is taken as the maximum uniaxial strength and the associated pressure value in SHPB tests. In Figure 8, all glass testing data are normalized against the pseudo HEL.

It is difficult to get the maximum hydrostatic tensile pressure T directly through experiment. In developing the original JH2 model, Holmquist et al. used the averaged glass tensile strength from static split-tensile tests as T. Comparing testing data in the tensile region, it is obvious that the original JH2 model overestimates the glass tensile strength.

Therefore, in the present study the glass hydrostatic tensile pressure is assumed to be two thirds of the averaged glass tensile strengths. It is to be noted that the JH2 model was initially developed to simulate ceramic material response to ballistic impacts. The glass behaviour in tensile zone is therefore not well described although the model has been very popularly used in simulating glass structure responses under blast and impact loads. Nonetheless, it should be noted that tri-axial tensile test data, especially those under dynamic tri-axial tension is not available yet. The adoption of 2/3 of the averaged uniaxial tensile strength for hydrostatic tensile pressure in this study, or using the averaged tensile strength in the Holmquist et al.'s work [22], is based on assumption only. Further modification might be necessary to derive more accurate glass strength under tri-axial tension should such testing data becomes available.

Figure 9 compares the intact strength curves of the original JH2 model and the modified JH2 model at reference strain rate $\dot{\varepsilon}_0 = 1.0\ s^{-1}$. As can be seen, glass intact strength of the original JH2 model is a lot higher than that derived from the testing data on samples from window glass in both the compressive and tensile regions. Obviously the original JH2 model over-predicts the strength of annealed glass commonly used for windows in building structures.

3.2 Damage model

The damage owing to glass fracture in the JH2 model is defined by

$$D = \sum \Delta\varepsilon_P / {\varepsilon_p}^f \tag{6}$$

where $\Delta\varepsilon_P$ is the plastic strain during a cycle of integration, and ${\varepsilon_p}^f$ is the plastic strain to fracture under constant pressure P,

$${\varepsilon_p}^f = D_1(P^* + T^*)^{D_2} \tag{7}$$

where D_1 and D_2 are material constants.

It is difficult to quantify glass damage and the material constants at fracture. Despite some experimental investigations in the literature on soda-lime glass fracture mechanism

[11], it is still hard to interpret the testing data, such as damage level, and derive glass strength reduction or damage constants explicitly. In the original JH2 model, iterative processes were used to determine glass fracture strength and damage constants, where numerical computations with varied strength at fracture and damage constants were performed until glass behaviour matched experimental results. The present study adopts Holmquist et al.'s material constants for fracture and damage. This is because although the glass intact strength is dependent on the glass surface treatment, the surface treatment is believed not to alter the glass material damage and fracture process. Therefore the damage model in the original JH2 model is still adopted here.

3.3 Strain rate effect

Figure 7 depicts dynamic increment effect on glass compressive and tensile strengths with respect to deformation rate. As noticed in Eq. (3) and (4), the JH2 model employs a logarithmic relation of DIF with strain rate to account for the dynamic amplification on both the intact strength and material strength at fracture. In the original model, the strain-rate constant C was determined using compressive tests at two strain rates only (quasi-static and $\dot{\varepsilon}$=250s^{-1}). With more experimental results covering a wider strain-rate range as described above, the strain-rate effect on annealed glass is refined and re-determined here for more accurate modelling of glass behaviour.

Figure 10 illustrates the method to determine the strain-rate constant C, which follows the procedure for float glass [22] and AlN [27]. The glass strengths at various strain rates from experimental tests are plotted using solid symbols. To not mess up the plot, only the strengths at five typical strain rates are shown in Figure 10. As shown, all these data fall on the straight line with stress-pressure ratio 3:1 since no additional confining pressure exists. Straight lines are drawn from the hydro tensile pressure T through these testing data. By definition the variation of slopes stands for strain-rate effect. In the JH2 model, material strength is both strain rate and pressure sensitive (as depicted in Eq. 3 and Eq. 4). Therefore,

to quantify the strain-rate effect, glass material strengths at different strain rates must be normalized to a constant pressure $P_{const.}$=79MPa as shown in Figure 10. These normalized glass strengths (open symbols) can then be incorporated with the corresponding strain rates. Similar to Figure 7, a bi-linear relation between equivalent stress and strain rate can be observed, where strain rate effect is less significant when $\dot{\varepsilon} \leq 100s^{-1}$ as compared with the data when $\dot{\varepsilon} > 100s^{-1}$. To fit in the format of the JH2 model, C=0.035 is obtained by averaging the strain rate constants in the two regions. As shown in Figure 10, the variation induced by combining these two strain rate constants is quite small (maximum variation less than 3%). This strain rate constant will be used in the JH2 model to represent the dynamic strength increment with strain rate. Nevertheless, it should be noted that to account for the bi-linear DIF-strain rate relation, a more sophisticated strain rate model is needed. This will be a possible topic of further study in the future.

The previous tests also found the glass tensile strength is highly strain rate dependent [21] as shown in Figure 7b, but the strain-rate effect on glass tensile strength is not considered in the original JH2 model. The original JH2 model adopted the averaged static tensile strength from split-tensile tests as cut-off pressure. In the present work, the dynamic amplification effect on glass material tensile strength is modelled by modifying the hydro tensile pressure according to the tensile DIF as described above at the corresponding strain rate.

3.4 Equation of state (EOS)

The equation of state for glass under compression is expressed as

$$P = K_1\mu + K_2\mu^2 + K_3\mu^3 + \Delta P \tag{8}$$

where K_1, K_2, K_3 are constants, and K_1 is the material bulk modulus. $\mu=\rho/\rho_0-1$, in which ρ is the current density and ρ_0 is the initial density.

$$U = \frac{\sigma^2}{6G} \tag{9}$$

$$\Delta U = U_{D(t)} - U_{D(t+\Delta t)} \tag{10}$$

In Eq. (8) the hydrostatic pressure is simply the first term before fracture happens; as damage initiates and accumulates, bulking tends to begin, which leads to the increment of pressure ΔP. The pressure increment is determined from energy consideration. The difference of internal elastic energy of deviator stress ΔU (Eq. 9 and Eq. 10) is converted to potential internal energy. The pressure increment can be solved as

$$\Delta P_{t+\Delta t} = -K_1 \mu_{t+\Delta t} + \sqrt{(K_1 \mu_{t+\Delta t} + \Delta P_t)^2 + 2\beta K_1 \Delta U} \tag{11}$$

The original EOS was derived by data fitting the pressure volume relationships from plate impact tests on three float glass specimens [22]. More experiments have been reported over the years on annealed soda-lime glass behaviour under shock loading in different pressure regions [17, 31, 32]. These testing data together with the original JH2 data are plotted in Figure 11. In the current study, the bulk modulus K_1 is calculated by

$$K_1 = \frac{E}{3(1-2\upsilon)} \tag{12}$$

where the Young's modulus E is 70GPa, which is averaged from the static compressive test data; υ is the Poisson's ratio which is assumed to be 0.23. With the bulk modulus K_1 determined, the coefficients K_2 and K_3 in the EOS equation (8) are then determined through best fitting the testing data in Figure 11. As shown the modified equation of state better matches the testing data on float glass pressure with respect to the material density. It can also be noted that although different surface conditions of glass specimens may influence glass ultimate compressive and tensile strengths, it would barely affect the material internal structure. In other words, surface treatment does not significantly affect the EOS of the glass material.

In summary, all the material constants derived are given in Table 3. These constants together with the DIF relations will be used to model the soda-lime glass material properties.

4 VERIFICATION OF MATERIAL MODEL

To verify the above model in predicting the dynamic responses of annealed soda-lime glass material and glass window panel, the model is programmed and linked to commercial program LS-DYNA [33] and used to predict three tests, namely a SHPB test on a glass specimen, a field blast test on a glass window, and a full-scale laboratory test on a glass window under windborne debris impact. The tests, numerical simulations and comparisons are presented in detail in the following section.

4.1 SHPB test

The SHPB test described above was replicated numerically to verify the accuracy of the glass material model (Figure 12a). The incident and transmitter bars are 1200mm in length and 20mm in diameter. Both pressure bars are constructed with maraging steel, and are simulated with elastic material model. Typical material parameters in the simulation are Young's modulus 210GPa, material density 8100kg/m^3, and Poisson's ratio 0.3. The glass specimen of dimension 15mm × 15mm (diameter × length), same as those tested is modelled. The JH2 model with material constants listed in Table 3 as well as the original material constants provided in reference [22] are used in the simulation to model glass material. Both pressure bars and glass specimen are modelled with three dimensional (3D) solid elements. Glass cylinder and steel bars near the contact areas with the glass specimen are meshed with denser elements. The mesh size convergence study is conducted. The convergence study finds that the element mesh size of 0.5mm × 0.5mm × 1.5mm for steel bars and 0.5mm × 0.5mm × 0.5mm for glass and bars near the contact regions give converged simulation of the SHPB tests. Further reducing the element size does not significantly improve the simulation results, but greatly increases the computation time. Therefore these mesh sizes are used in the subsequent simulations. AUTOMATIC_SURFACE_TO_SURFACE contact in LS-DYNA is used to model the ideal smooth contact between glass specimen and incident and transmitter bars. Since the simulation

focuses on the behaviour of glass response, a stress impulse recorded on incident bar in the laboratory test is applied as a stress boundary (Figure 12b) to the incident bar without modelling the strike bar to simplify the numerical simulation.

Figure 13 illustrates the stress time histories recorded in the incident and transmitter bars. For comparison, bar stresses from numerical simulations with both the modified and the original JH2 material constants are presented. As can be seen, the reflected and transmitted stresses from the modified model match reasonably well with those from experimental test. As shown, the transmitted stress obtained with the modified model drops quickly after its peak stress, while the stress recorded in the experimental test decreases gradually. The difference can be attributed to the friction existing between glass specimen and steel bars, which affects the damaged glass strength in the experimental test. Since the level of friction is hard to be predicted, it is not considered in the numerical computation. Both the original and modified models accurately predict the incident wave, but the original JH2 model greatly under predicts the reflected wave and over predicts the transmitted wave, because the original JH2 model overestimates annealed soda-lime glass compressive strength. The modified model gives better simulation of the SHPB test.

Figure 14 plots the true stress vs. true strain curves of the glass specimens. Glass strain in the experiment was measured using strain gauge glued on the specimen. It can be found that the numerical result with the modified JH2 constants reasonably simulates the glass behaviour. The simulated glass ultimate compressive strength and the corresponding strain closely match those in the laboratory test. An ultimate compressive strength of 703MPa is measured in the SHPB test, while a marginally higher value of 708MPa is predicted in the numerical simulation. On the contrary, the original JH2 model predicts higher maximum glass compressive strength (about 1190MPa) and higher strain. These comparisons demonstrate that the modified JH2 model better predicts the annealed soda-lime glass

material behaviour in SHPB tests than the original model, which overestimates float glass strength.

4.2 Blast test

The numerical model is also used to simulate responses of laminated glass windows to air blast load. A 3D model of laminated glass panel is developed to replicate Hooper et al.'s free field blast test [34]. As shown in Figure 15a, the window is 1.5m × 1.2m with all sides fully clamped using steel strips. The laminated glass is 7.52mm thick, i.e. two layers of 3mm annealed glass laminating a 1.52mm PVB interlayer. Only one quarter of glass panel with steel frame is modelled due to symmetry. The frame is made of 20mm wide, 6mm thick mild steel strips. Elastic material model is adopted for steel frame with density 7800kg/m^3, Young's modulus 208GPa and Poisson's ratio 0.3. The laminated glass is meshed with 2-element each layer through its thickness. In-plane mesh size is checked for numerical convergence, which yields 3mm × 3mm × 1.5mm mesh for glass and 3mm × 3mm × 0.76mm mesh for PVB. The steel strip is meshed with 6 elements in the width direction, 2 elements in the thickness direction, and 3mm element size in its length direction. Both the modified and the original JH2 models are used for glass material separately in the simulations to demonstrate the improvement in simulation accuracy. The interlayer material PVB is modelled using a strain-rate dependent elastic-plastic material model described in reference [4]. The accuracy of this model was examined exclusively; hence it is not elaborated here. Erosion is used to model glass crack, and to allow for the rupture of interlayer. Erosion criterion is 0.03 of the maximum principal strain of glass. This criterion is selected considering the fact that glass material is very brittle under tension. When thin plate like glass windows is subjected to transverse loads, tensile failure is predominant rather than shear failure. PVB element is subjected to erosion when the maximum principal strain reaches 2.0 according to the experimental study on PVB ultimate tensile capacity. All eroded elements lose load-carrying capacity but are retained so as to maintain mass and energy

conservations. AUTOMATIC_SURFACE_TO_SURFACE_TIEBREAK model is used to simulate adhesion contact between glass ply and PVB interlayer, where 10MPa shear strength and 10MPa tensile strength are used. In the test described in reference [34], 15kg TNT equivalent charge was detonated at 13m stand-off distance. Recorded blast pressure is shown in Figure 15b together with the fitted blast loading time history that is applied to the outer glass ply in this study. The negative phase is also considered in the simulation.

The recorded and simulated displacement histories at the centre of glass panel are compared in Figure 16. As shown the numerical simulation with the modified JH2 model for glass reasonably reproduces the experimental test of the glass window. The original JH2 model predicts a very small mid span deflection (48mm), which is because it overestimates the glass material strengths. Relatively large displacement is induced in the glass panel because after glass damage, its deformation is governed by PVB layer with relatively low stiffness. The maximum displacement of the numerical simulation (184mm) is slightly higher than that of the experimental test (173mm). This could be attributed to the uncertainties of the PVB material model and the test conditions. The comparisons indicate that the modified JH2 model gives a reasonable prediction of glass window damage to blast loads.

4.3 Windborne debris impact

Laboratory test on windborne wood debris impact against laminated glass reported in reference [3] is numerically simulated to further demonstrate the accuracy of the modified model (Figure 17). A 7.88mm laminated glass window (3mm glass, 1.88mm PVB interlayer and 3mm glass) is built using 3D solid elements with verified mesh sizes (3mm × 3mm × 1.5mm for glass and 3mm × 3mm × 0.94mm for PVB). The window frame of 15mm × 6mm (width × thickness) aluminium strips are modelled using 3mm × 3mm × 3mm solid elements to constrain glass panel. Without any sign of aluminium material yielding in the laboratory tests after impacting, elastic material model is chosen for aluminium frame with density 2700kg/m^3, Young's modulus 70GPa and Poisson's ratio 0.3. A 4kg hard pine projectile with

an impact area of 100mm × 50mm is launched at a speed of 15m/s targeting at the centre of the laminated glass window. The wood density and Young's modulus are 500kg/m^3 and 9GPa respectively. The wood block is meshed into 5mm × 5mm × 5mm solid elements. PVB material model and adhesion between interlayer and glass are the same as described above in section 4.2. Only one quarter model is generated owing to symmetry to save computer memory and reduce computational time. The original and modified JH2 models are used for float glass pane to evaluate their accuracy in simulating the response of laminated glass window subjected to windborne debris impact.

Glass window behaves differently under windborne debris impact (as depicted in Figure 18) compared to that under blast loading. Glass experiences very concentrated impact energy at the location where the wood projectile impacts. Glass at the impact region is shattered or even smashed under the impact. Damage extends through glass panel. The damaged glass panel is held by the PVB interlayer, and is pushed by the travelling projectile until all kinetic energy is dissipated through breakage of glass panel and deformation of interlayer. Glass cracks are formed and developed as the panel deforms. Unlike the situation under blast loading, glass shatters into finer fragments near the impact zone and cracks get less and less dense as they extend towards the boundary. Figure 18 compares the damage processes of outer glass panes in numerical simulations with the original and modified JH2 models. It can be observed that at the time when the wood projectile strikes at the panes (t=0.3ms) the original JH2 model predicts very limited glass damage due to the overestimated glass strength, while the damage contour of the modified glass model shows severe glass damage at the impact surface. As the projectile pushes glass pane inwards, glass damage extends radially towards window boundaries. In contrast, the original JH2 model only predicts a couple of severe cracks initiated next to the projectile impact location, which are resulted from flexural and shear deformations. These cracks spread outwards but are associated with few minor glass damages. Comparing the numerical simulations with

laboratory tested glass pane in Figure 19, it can be found that the numerical simulation with the modified glass material model manages to capture the crush of glass at the debris impact zone, as well as glass damage in the outer glass pane. In comparison, the original JH2 model could not give accurate estimation of glass window behaviour under debris impact.

The mid-point deflection of the glass window in the experiment was monitored by high-speed camera, which was post processed with a tracking algorithm to form the deflection time history (shown in Figure 20). The glass window central deflection histories predicted are presented in the figure as well. As comparison indicates, the simulated maximum pane deflection using the original JH2 model (58mm) differs significantly from the maximum pane deflection in the laboratory test (118mm). This is mainly because the glass material strength was overestimated. As shown above in Figure 18, very limited glass was damaged under compression in the outer pane. The strong window pane rebounds quickly after it reaches its maximum deflection at about 6ms. The maximum deflection from numerical simulation with the modified JH2 model (132mm) matches closely with that in the laboratory test. The numerical result is slightly larger than the experimental data. The difference could be attributed to two possible reasons, namely the difference in boundary conditions and the idealized wood projectile model. In the laboratory test, a very thin layer of silicone glue was squeezed in the gap between the aluminium frame and glass pane to avoid pre-test damage of glass during transportation and installation. This is not modelled in numerical simulation and direct contact between glass and frame is assumed. Secondly, the idealized wood projectile model could also lead to some error in the predicted window deflection. Wood is a complicated material, which is anisotropic and porous. In the current simulation, considering the hard pine used in the laboratory test, an elastic material model is adopted for wood to simplify the modelling and simulation effort. This might result in overestimation of the interaction between wood projectile and glass windows, which consequently leads to the overestimated glass pane deflection. Nevertheless, through comparisons on glass damage,

pane cracking and panel displacement with laboratory test results, numerical simulation conducted with the modified JH2 material model for glass gives good predictions of laminated glass response in windborne debris impact.

5 CONCLUSIONS

This paper presents material constants for the popular brittle material model - JH2 model for annealed soda-lime glass used in architectural windows. New quasi-static compressive tests and dynamic compressive tests with SHPB device were performed to investigate the annealed glass properties at high strain rates. Together with previous material testing data, material constants for JH2 model for annealed soda-line glass were derived. The accuracy of the modified JH2 model for glass material was verified with a SHPB compressive test, a field blast test, and a laboratory impact test on laminated glass windows. The accuracy of the modified model and the original JH2 model in simulating glass responses to dynamic loads were checked through numerical simulations. The results indicated that the modified JH2 model was capable of representing annealed soda-lime glass properties and giving reasonable predictions of glass window responses to shock and impact loads.

ACKNOWLEDGMENT

The authors would like to thank Australian Research Council for financial support. The first author would also like to thank the University of Western Australia for providing Ad Hoc scholarship.

REFERENCE

[1] Wikipedia, Norway Attacks, 2011, http://en.wikipedia.org/wiki/2011_Norway_attacks.
[2] G. Walker, The Application of Wind Engineering Technology to the Mitigation of Damage to Housing from Tropical Cyclones-An Australian Achievement, International Conference on Impact of Disasters, Los Angeles, USA, 1991.
[3] X. Zhang, H. Hao, G. Ma, Laboratory test and numerical simulation of laminated glass window vulnerability to debris impact, International Journal of Impact Engineering, 55 (2013) 49-62.
[4] X. Zhang, H. Hao, G. Ma, Parametric study of laminated glass window response to blast loads, Engineering Structures, 56 (2013) 1707-1717.

[5] M. Timmel, S. Kolling, P. Osterrieder, P.A. Du Bois, A finite element model for impact simulation with laminated glass, International Journal of Impact Engineering, 34 (2007) 1465-1478.
[6] M. Larcher, G. Solomos, F. Casadei, N. Gebbeken, Experimental and numerical investigations of laminated glass subjected to blast loading, International Journal of Impact Engineering, 39 (2012) 42-50.
[7] J. Wei, M.S. Shetty, L.R. Dharani, Failure analysis of architectural glazing subjected to blast loading, Engineering Failure Analysis, 13 (2006) 1029-1043.
[8] X. Zhang, H. Hao, Z. Wang, Experimental investigation of monolithic tempered glass fragment characteristics subjected to blast loads, Engineering Structures, 75 (2014) 259-275.
[9] L.H. Lin, E. Hinman, H.F. Stone, A.M. Roberts, Survey of Window Retrofit Solutions for Blast Mitigation, Journal of Performance of Constructed Facilities, 18 (2004) 86-94.
[10] S. Chocron, K. Dannemann, J. Walker, A. Nicholls, C. Anderson Jr, Static and dynamic confined compression of Borosilicate glass, in: Proceedings of Proceedings of the DYMAT conference, Belgium, 2009.
[11] K.A. Dannemann, C.E. Anderson, S. Chocron, J.F. Spencer, Damage Development in Confined Borosilicate and Soda-Lime Glasses, Journal of the American Ceramic Society, 95 (2012) 721-729.
[12] K.A. Dannemann, S. Chocron, A.E. Nicholls, C.E. Anderson Jr, Compressive damage development in confined borosilicate glass, Materials Science and Engineering: A, 478 (2008) 340-350.
[13] X. Nie, W.W. Chen, X. Sun, D.W. Templeton, Dynamic Failure of Borosilicate Glass Under Compression/Shear Loading Experiments, Journal of the American Ceramic Society, 90 (2007) 2556-2562.
[14] X. Nie, W. Chen, High-Rate Progressive Failure of Borosilicate Glass under Mechanical Confinement at High Temperatures, Experimental Mechanics, (2012) 1-9.
[15] X. Nie, W.W. Chen, A.A. Wereszczak, D.W. Templeton, Effect of Loading Rate and Surface Conditions on the Flexural Strength of Borosilicate Glass, Journal of the American Ceramic Society, 92 (2009) 1287-1295.
[16] N. Bourne, J. Millett, Z. Rosenberg, N. Murray, On the shock induced failure of brittle solids, Journal of the Mechanics and Physics of Solids, 46 (1998) 1887-1908.
[17] C. Alexander, L. Chhabildas, W. Reinhart, D. Templeton, Changes to the shock response of fused quartz due to glass modification, International Journal of Impact Engineering, 35 (2008) 1376-1385.
[18] M. Grujicic, W. Bell, B. Pandurangan, B. Cheeseman, C. Fountzoulas, P. Patel, D. Templeton, K. Bishnoi, The effect of high-pressure densification on ballistic-penetration resistance of a soda-lime glass, Proceedings of the Institution of Mechanical Engineers, Part L: Journal of Materials Design and Applications, 225 (2011) 298-315.
[19] Z. Rosenberg, Y. Ashuach, E. Dekel, More on the behavior of soda lime glass under shock loading, International Journal of Impact Engineering, 35 (2008) 820-828.
[20] M. Peroni, G. Solomos, V. Pizzinato, M. Larcher, Experimental Investigation of High Strain-Rate Behaviour of Glass, Applied Mechanics and Materials, 82 (2011) 63-68.
[21] X. Zhang, Y. Zou, H. Hao, X. Li, G. Ma, K. Liu, Laboratory Test on Dynamic Material Properties of Annealed Float Glass, International Journal of Protective Structures, 3 (2012) 407-430.
[22] T.J. Holmquist, G.R. Johnson, C. Lopatin, D. Grady, E.S. Hertel Jr, High strain rate properties and constitutive modeling of glass, in: Proceedings of 15th International Symposium on Ballistics Jerusalem, Israel, 1995.
[23] M. Grujicic, B. Pandurangan, W. Bell, B. Cheeseman, C.-F. Yen, C. Randow, Molecular-level simulations of shock generation and propagation in polyurea, Materials Science and Engineering: A, 528 (2011) 3799-3808.

[24] G. Camacho, M. Ortiz, Computational modelling of impact damage in brittle materials, International Journal of Solids and Structures, 33 (1996) 2899-2938.
[25] M. Grujicic, B. Pandurangan, W.C. Bell, N. Coutris, B.A. Cheeseman, C. Fountzoulas, P. Patel, D.W. Templeton, K.D. Bishnoi, An Improved Mechanical Material Model for Ballistic Soda-Lime Glass, Journal of Materials Engineering and Performance, 18 (2009) 1012-1028.
[26] X. Zhang, H. Hao, Laboratory Test and Numerical Simulation of Laminated Glass Window Response to Impact and Blast Loads, in: Proceedings of the 9th International Conference on Shock & Impact Loads on Structures, Fukuoka, Japan, 2011.
[27] T.J. Holmquist, D.W. Templeton, K.D. Bishnoi, Constitutive modeling of aluminum nitride for large strain, high-strain rate, and high-pressure applications, International Journal of Impact Engineering, 25 (2001) 211-231.
[28] G.R. Johnson, T.J. Holmquist, S.R. Beissel, Response of aluminum nitride (including a phase change) to large strains, high strain rates, and high pressures, Journal of Applied Physics, 94 (2003) 1639-1646.
[29] T.J. Holmquist, G.R. Johnson, A Computational Constitutive Model for Glass Subjected to Large Strains, High Strain Rates and High Pressures, Journal of Applied Mechanics, 78 (2011) 051003.
[30] G.R. Johnson, T.J. Holmquist, An improved computational constitutive model for brittle materials, in: Proceedings of AIP Conference Proceedings, 1994.
[31] D. Dandekar, P. Beaulieu, Failure wave under shock wave compression in soda lime glass, Metallurgical and Material Applications of Shock-Wave and High-Strain-Rate Phenomena, (1995) 211-218.
[32] D.E. Grady, L.C. Chhabildas, Shock-wave properties of soda-Lime glass, Sandia National Labs., Albuquerque, , NM, United States (1996).
[33] LS-DYNA® Version 971 User's Manual, Livermore Software Technology Corporation, 2007.
[34] P.A. Hooper, R.A.M. Sukhram, B.R.K. Blackman, J.P. Dear, On the blast resistance of laminated glass, International Journal of Solids and Structures, 49 (2012) 899-918.

Specimen No.	Maximum Strength (MPa)	E (GPa)
1	223.0	53.2
2	237.1	56.4
3	250.0	60.2
Mean	236.7	56.6
Std. Dev.	13.5	3.5

Table 1 Static compressive test results

Specimen No.	True strain rate (s^{-1})	Maximum Strength (MPa)
1	619	718
2	644	560
3	675	703
4	936	842
5	953	874
6	813	825
7	1464	968
8	1465	959
9	1369	1003
10	1314	990

Table 2 SHPB compressive test results

Density (kg/m^3)	2530
Strength Constants	
A	0.75
B	0.2
C	0.035
M	1.0
N	0.72
Tensile strength (MPa)	27.8
Pseudo HEL (MPa)	1003
Normalized fracture strength	0.5
HEL strength (MPa)	334
Shear modulus (GPa)	26.9
Damage Constants	
D1	0.043
D2	0.85
Equation of State	
K1 (GPa)	43.2
K2 (GPa)	-67.2
K3 (GPa)	153.2
Bulk	1.0

Table 3 Material constants for annealed soda-lime glass

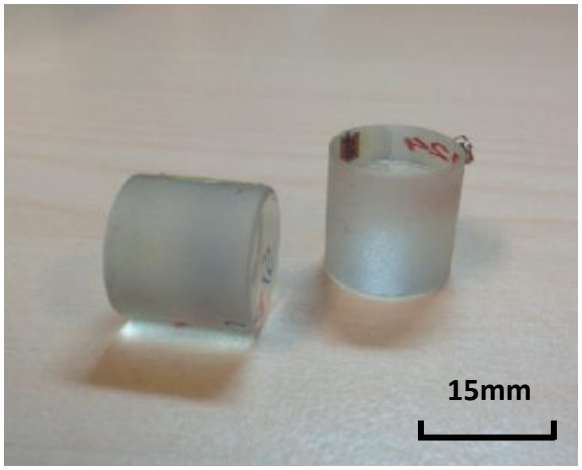

Figure 1 Glass specimens

Figure 2 INSTRON quasi-static compressive testing machine

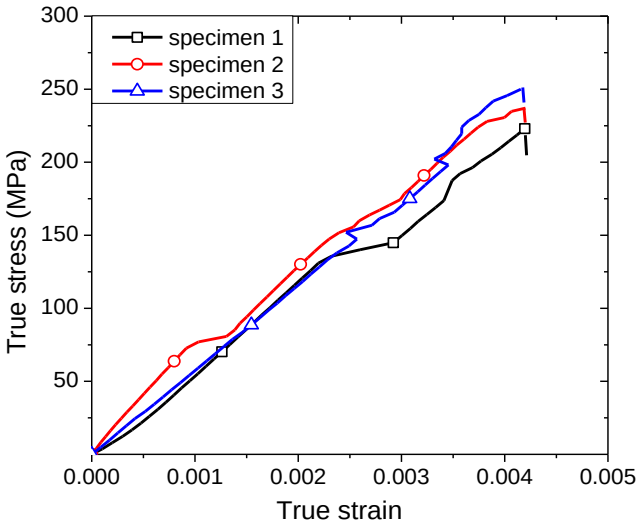

Figure 3 True stress-strain curves of glass under static compression

Figure 4 SHPB device used in the current study

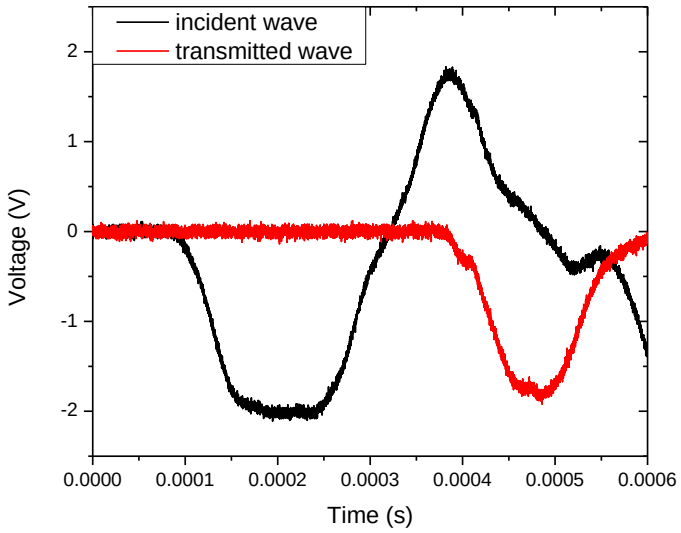

Figure 5 Typical incident and transmitted waves recorded in the tests

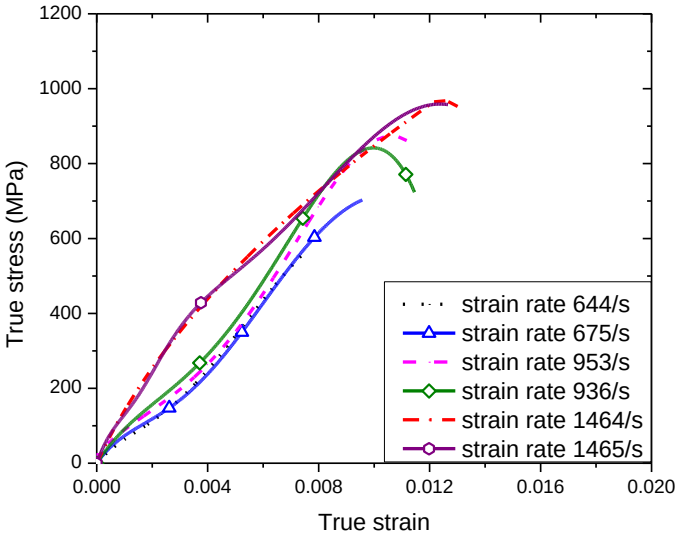

Figure 6 Typical true stress-strain curves from dynamic compressive tests

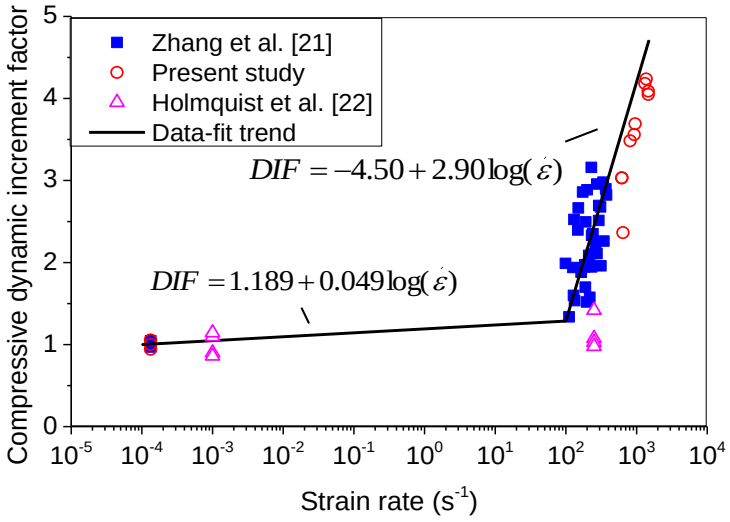

a) Compressive dynamic increment factors vs. true strain rates

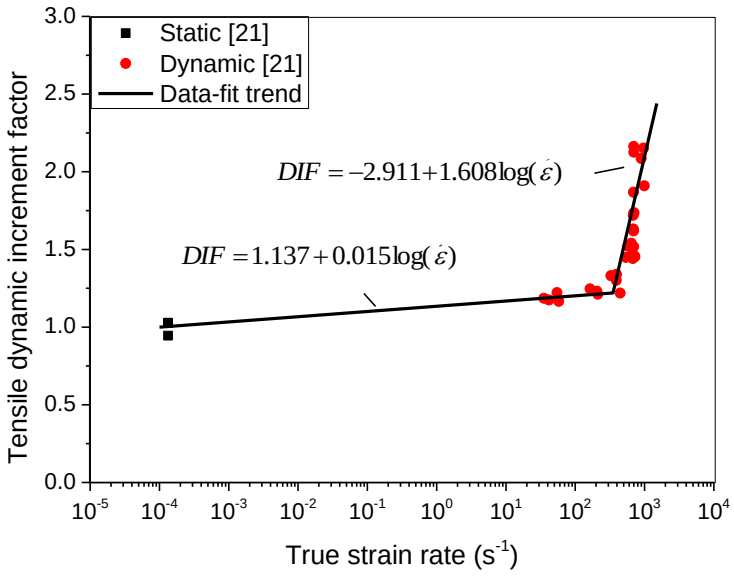

b) Tensile dynamic increment factors vs. true strain rates in reference [21]

Figure 7 Glass compressive and tensile dynamic increment factors vs. true strain rates

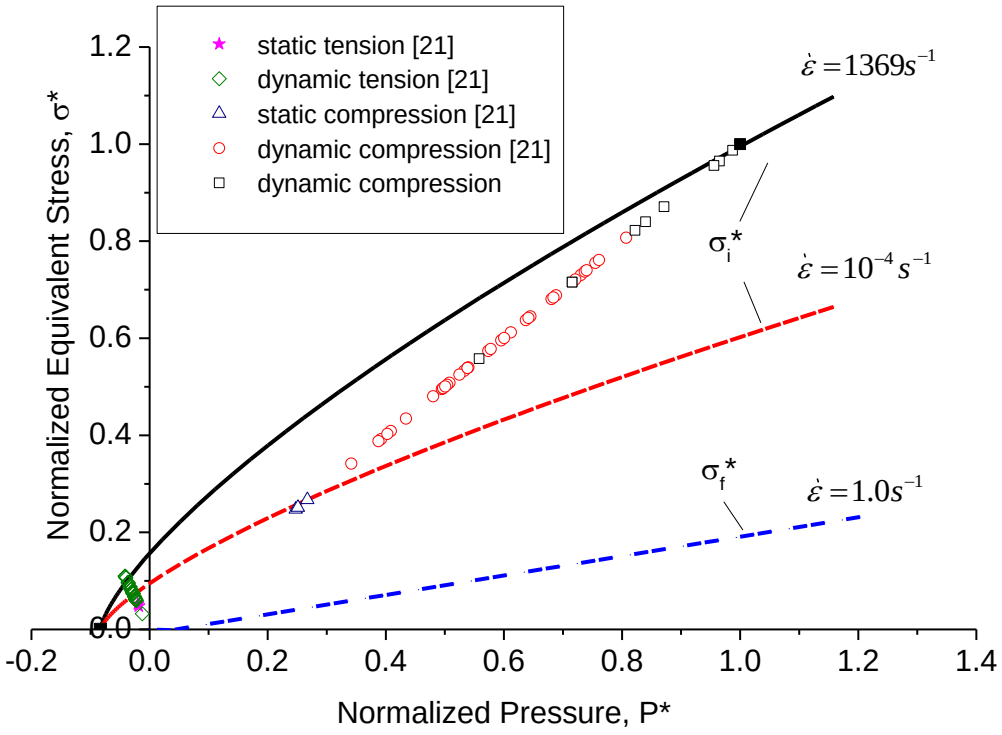

Figure 8 Glass strength model with testing data from the current study and reference [21]

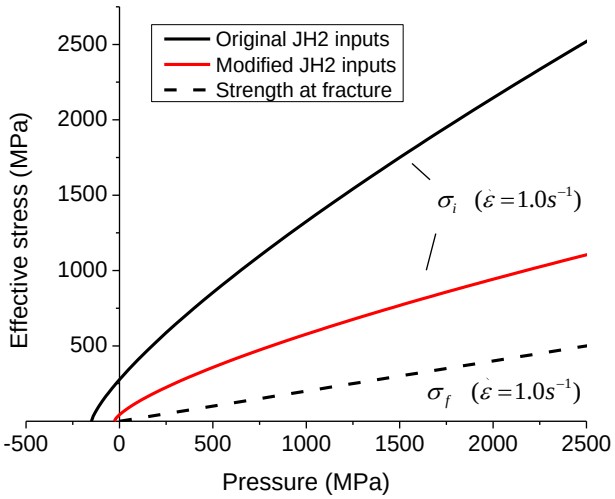

Figure 9 Comparison of the original and modified JH2 strength models

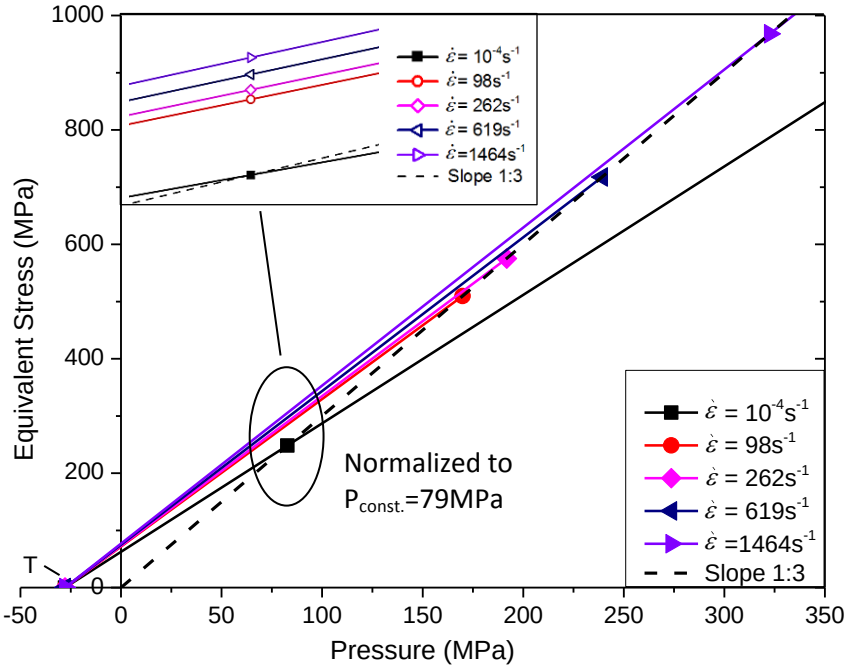

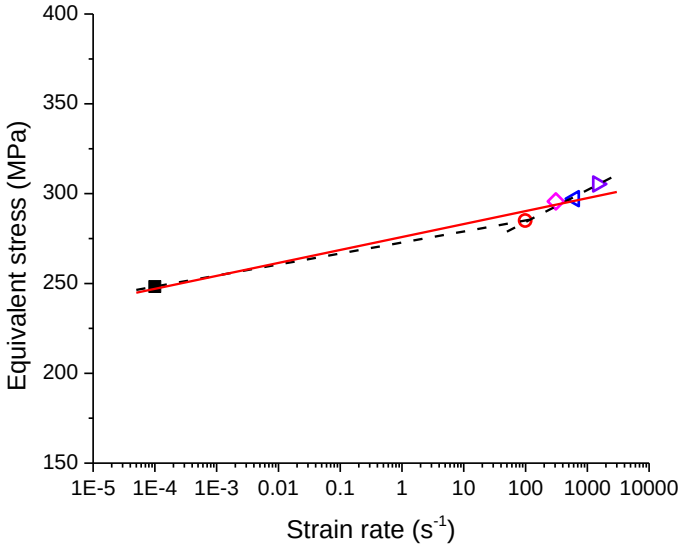

Figure 10 Strain rate sensitivity and determination of the constant for the strain rate effect model

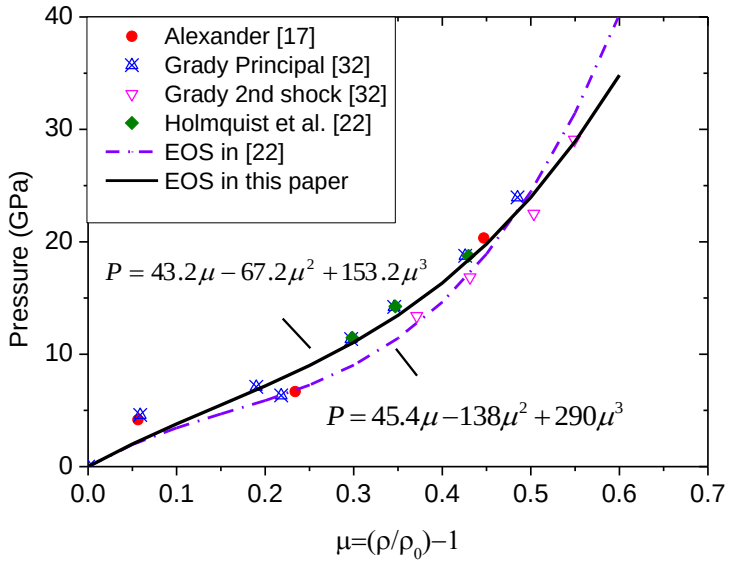

Figure 11 Test data for determination of material constants for Equation of state

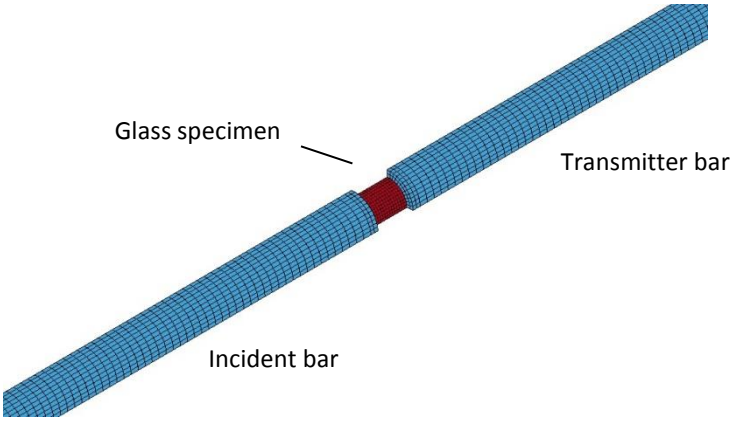

a) Numerical model

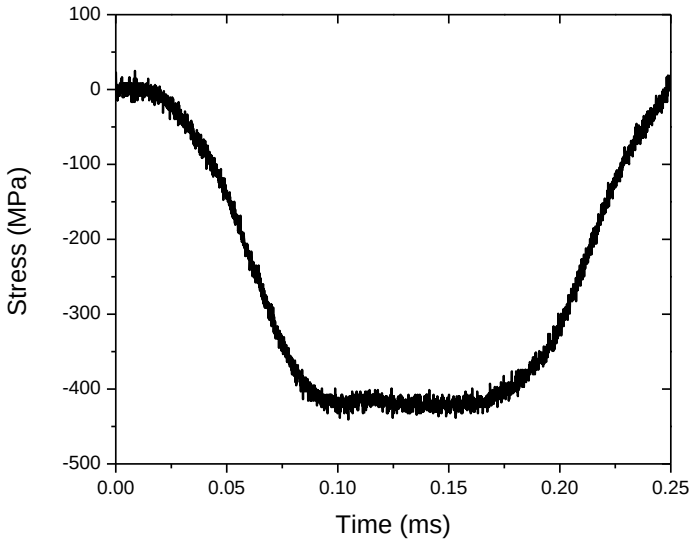

b) Recorded stress impulse in the test

Figure 12 Schematic numerical model of SHPB test

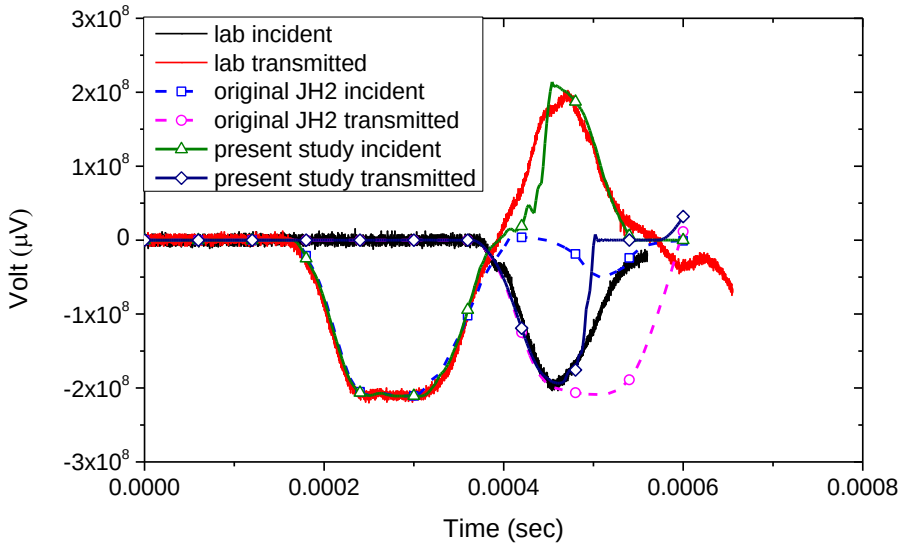

Figure 13 Comparison of stress waves in compressive SHPB test

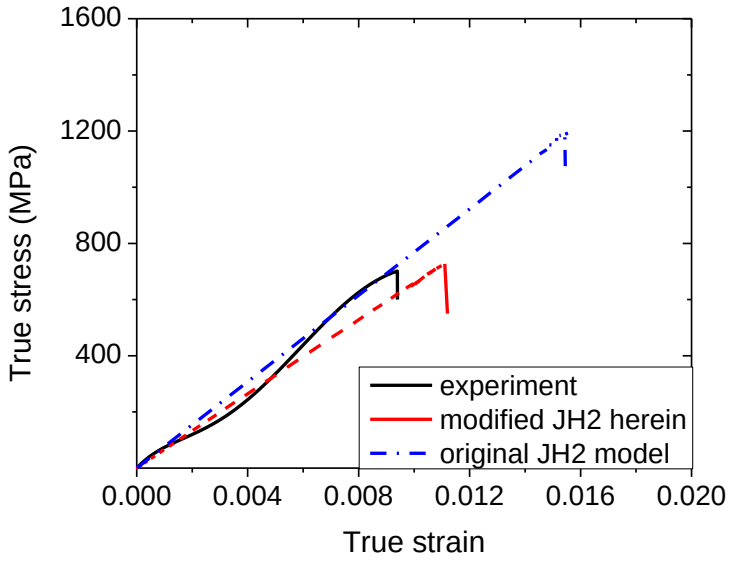

Figure 14 Comparison of true stress versus true strain curves from experimental test and numerical simulations

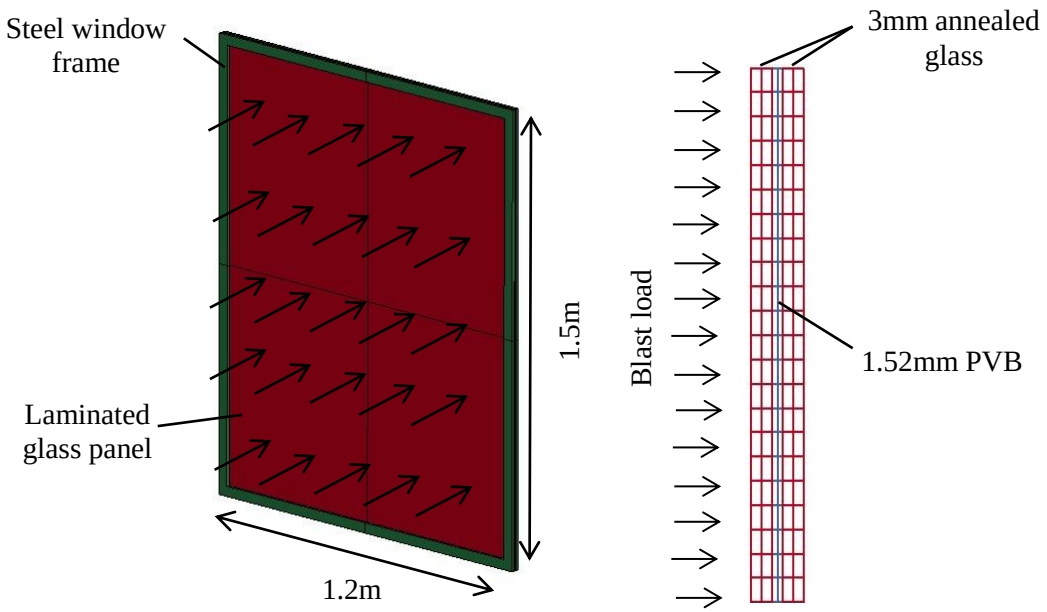

a) Laminated glass model

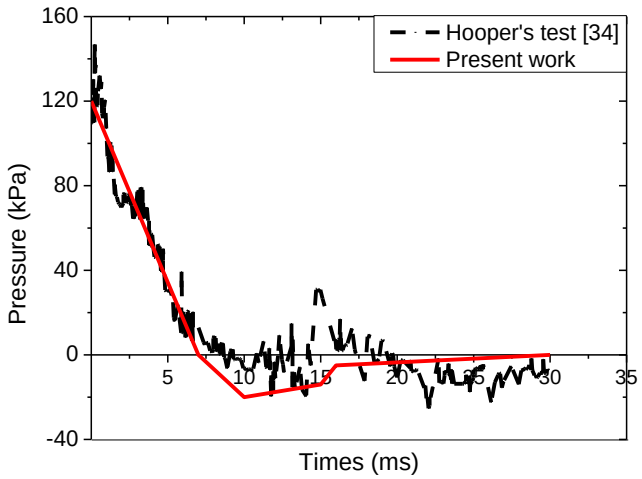

b) Pressure time history in [34] and blast load applied in numerical simulation

Figure 15 Schematic laminated glass model and blast load time history

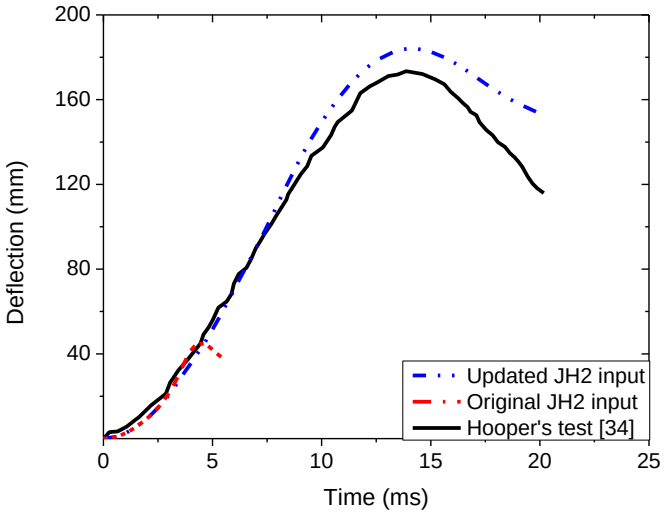

Figure 16 Comparison of the deflection histories obtained from numerical simulations and Hooper's experiment test [34]

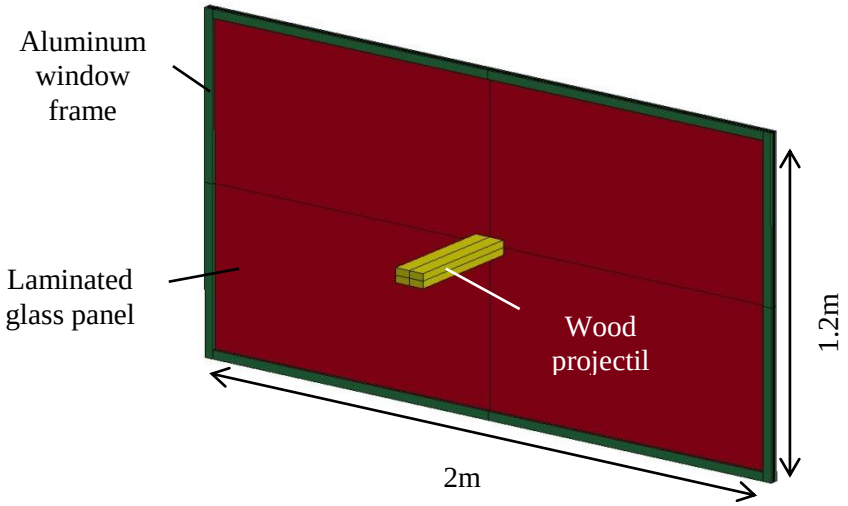

Figure 17 Model of debris impact on laminated glass window

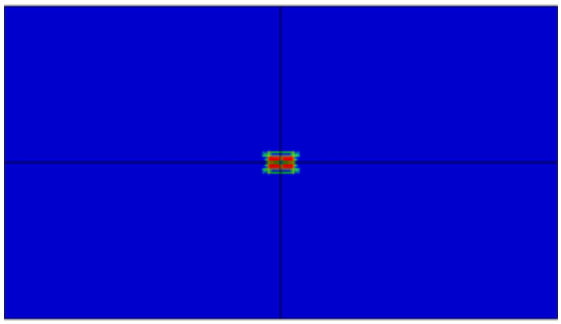

t=0.3ms

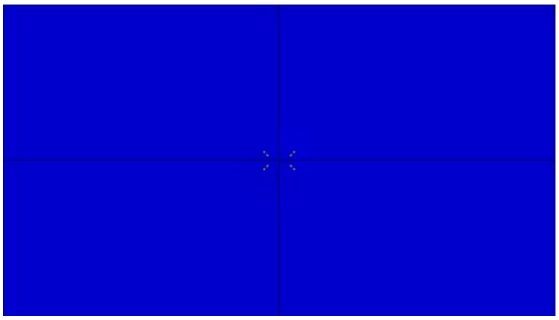

t=0.3ms

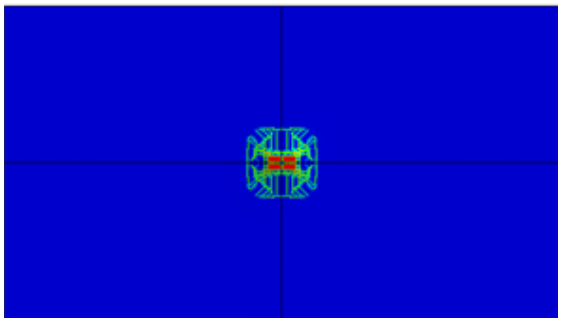

t=3ms

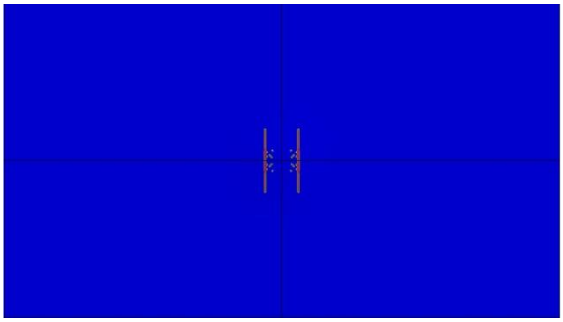

t=3ms

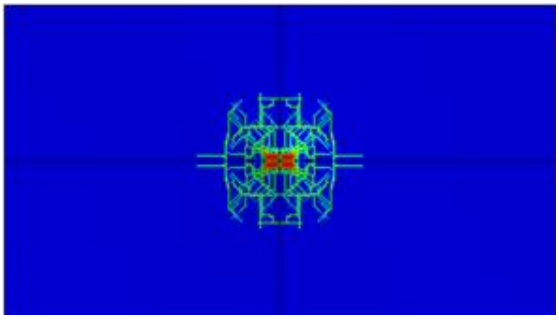

t=5ms

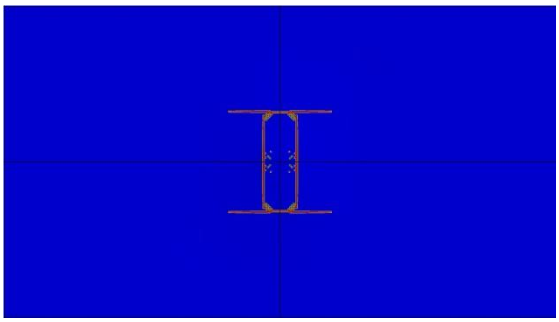

t=5ms

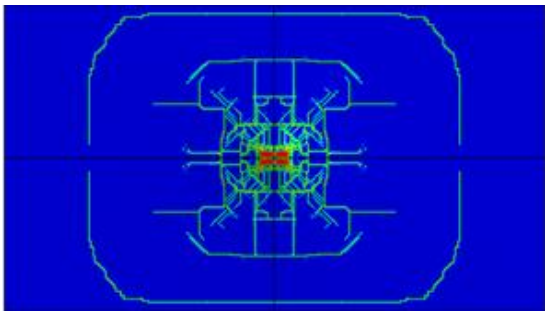

t=12ms

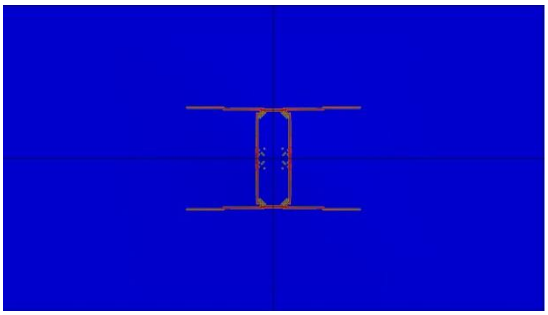

t=7ms

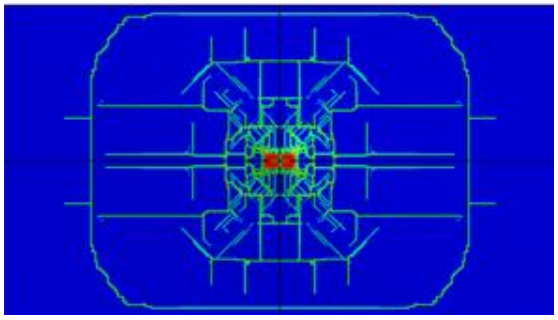

t=28ms

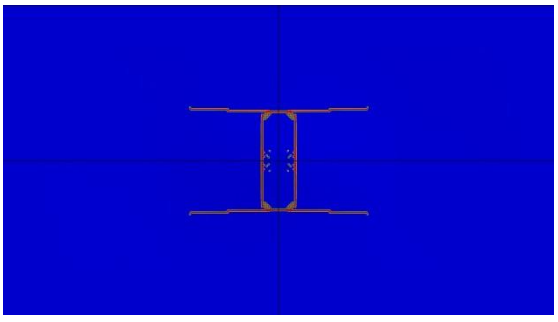

t=17ms

a) Updated JH2 input b) Original JH2 input

Figure 18 Comparison of glass damage processes

Figure 19 Damaged glass pane in laboratory test

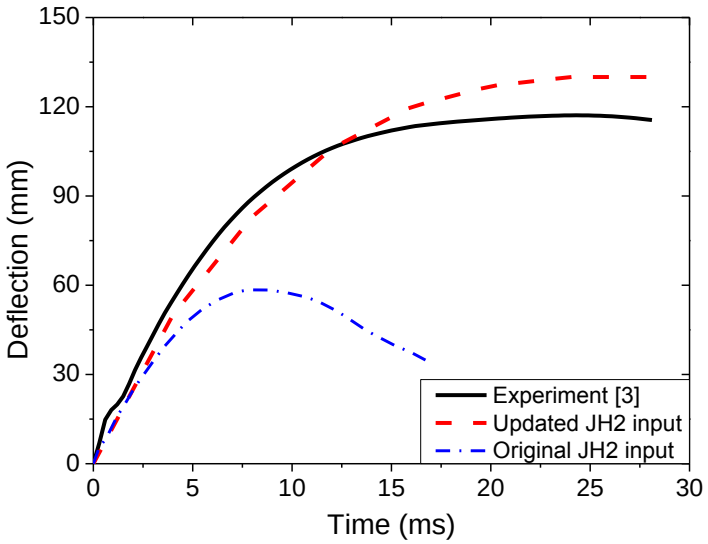

Figure 20 Windows central-point deflection time histories